DOI 10.1007/s11041-023-00915-0
Metal Science and Heat Treatment, Vol. 65, Nos. 3 – 4, July, 2023 (Russian Original Nos. 3 – 4, March – April, 2023)

UDC 669.14:669.15:194.55:621.789

SPECIAL FEATURES OF THE $\alpha \rightarrow \gamma$ TRANSFORMATION OF RADIALLY FORGED LOW-CARBON STEEL IN THE INTERCRITICAL TEMPERATURE RANGE

T. Yu. Barsukova,[1] D. O. Panov,[1] Yu. N. Simonov,[1] A. S. Pertsev,[1] V. Ts. Toshkov,[1] and A. V. Il'inykh[1]

Translated from *Metallovedenie i Termicheskaya Obrabotka Metallov*, No. 4, pp. 13 – 20, April, 2023.

Original article submitted May 6, 2022.

The effect of cold radial forging of steel 10Kh3G3MFS in a two-phase martensitic-ferritic state on the kinetics of formation of austenite under subsequent heating at different rates is studied. The quantitative characteristics of the stages of formation of the austenite are determined and a thermokinetic diagram of the austenitization is plotted. The parameters of the martensitic-ferritic structure and of the hardness of the steel are shown to depend on the temperature of quenching from the intercritical temperature range. The influence of preliminary radial forging on the behavior of the curves of uniaxial tension of the steel after incomplete quenching is studied and compared to the results obtained earlier for a quenched condition.

Key words: low-carbon steel, austenitization, dilatometry, kinetics, incomplete quenching, intercritical temperature range, microstructure, mechanical properties.

INTRODUCTION

Low-carbon nickel-free steels of type Kh3G3MF with Ti, V and Si additions exhibit high stability of supercooled austenite, which provides a structure of low-carbon martensite upon air cooling in up to 100-mm sections [1]. In a heat-refined condition, the mechanical properties of such steels are close to those of medium-carbon low-alloy ones.

Heat treatment for raising the structural strength low-carbon steels of martensitic class should be applied with allowance for their high tempering resistance and susceptibility to structural inheritance. These properties are a result of preservation of the packet-lath structure of the α-phase above the temperature of the start of the polymorphic transformation in them [2 – 4]. For this reason, the steels capable to harden in air are subjected to thermocycling [5, 6] including a hold in the intercritical temperature [ICTR] [7]. This makes it possible to obtain nanostructured packet martensite and provides simultaneous growth of the strength and impact toughness. If the strength of the steel exceeds the level required for service of the article, it is expedient to reduce it by forming a low content of a plastic phase, i.e., retained austenite or ferrite. The presence of such structural component will raise the ductility and the reliability of the steel. For example, the formation of metastable austenite in the structure of carbide-free bainite of steels (30 – 45)Kh3G3MFS due to isothermal quenching raises their ductility and toughness [8]. For martensitic steels containing less than 0.15% C quenching may be conducted from the upper part of the ICTR in order to preserve untransformed ductile α-phase in the structure.

It has been shown experimentally that the level of impact toughness in steel 10Kh3G3MFS increases in quenching from 800°C whatever its initial condition (quenched [9] or radially forged [10]), which requires scientific explanation. It should be noted that quenching of this steel yields a structure represented by a preserved matrix α-phase and freshly hardened martensite. Therefore, it is important to consider the effect of the initial condition on the phase composition of the steel after quenching from various temperatures and at various heating rates and on the morphology of the old and new

[1] Perm National Research Polytechnic University, Perm, Russia (e-mail: barsukova-chernova.tatyana@mail.ru).
[2] Belgorod State National Research University, Belgorod, Russia.
[3] Perm Scientific Research Technological Institute, Perm, Russia.
[4] Technological University-Sofia, Sofia, Bulgaria.

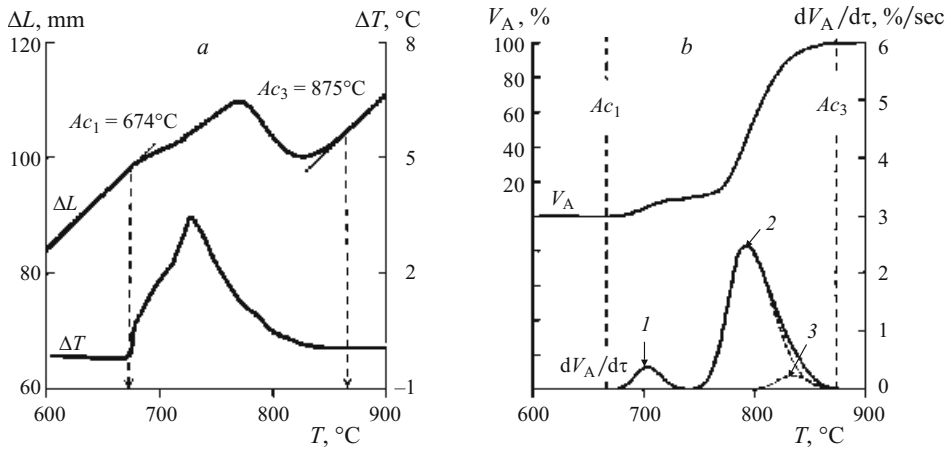

Fig. 1. Dilatometric curves of steel 10Kh3G3MFS in state *3*: *a*) variation of the length ΔL and of the temperature difference ΔT of the heater and of the sample under heating; *b*) critical kinetic curve of formation of austenite V_A and derivative of the kinetic curve $dV_A/d\tau$ for the heating rate of 1.5 K/sec with decomposition into peaks *1* (703°C), *2* (790°C) and *3* (834°C).

α-phase. It should be noted that the number, the size, and the shape of the austenite regions is inherited by martensite during the quenching cooling and will determine the strength properties of the steel. The features of the evolution of the structure of the matrix α-phase during the heating and the holding in the ICTR determine the influence of this structural component on the strength and ductility of the steel.

The aim of the present work was to study the special features of formation of austenite in steel 10Kh3G3MFS and to determine the effect of the preliminary treatment on the level of mechanical properties after quenching from the intercritical temperature range.

METHODS OF STUDY

We studied steel 10Kh3G3MFS of the following chemical composition (in wt.%): 0.10 C, 2.75 Cr, 2.51 Mn, 1.25 Si, 0.40 Mo, 0.12 V, 0.008 S, 0.019 P. The ingots with a mass of 40 kg were subjected to free hot forging within 950 – 1150°C to obtain rods with diameter 19 mm and then cooled in air (state *1*). The microstructure of the steel after the cooling was represented by low-carbon martensite [9]. Then the samples were placed in a furnace heated to 800°C (the ICTR), held for 2 h, and quenched in air (state *2*). As a result of such quenching the steel acquired a multiphase structure consisting of packet martensite with a low content of austenite and layers of an α-phase [9]. After the quenching, a part of the samples was subjected to a 60% deformation treatment, i.e., cold radial forging (CRF), in a radial compaction machine with continuous cooling of the deformation source with room-temperature water (state *3*). The radial forging was conducted at the following parameters: speed of feeding of the billet 180 mm/min, speed of its rotation 25 rpm, striker frequency 1000 impacts per minute. This treatment yielded a banded structure with a high dislocation density [11].

The samples in state *3* with a size of ∅3 × 10 mm were subjected to a dilatometric analysis using a Linseis R.I.T.A. L78 quenching dilatometer. A part of the samples was heated to 1000°C at a rate of 0.15, 0.6, 1.5, 20 and 90 K/sec and held for 8 sec. The other part was heated at a rate of 1.5 K/sec to 715, 750, 775, 800 and 860°C. The hold in the ICTR lasted for 6 h. The rate of cooling to room temperature was 50 K/sec. The measurements were made in an environment of high-purity helium. The content of the austenite in the ICTR under continuous heating and isothermal holds was determined using the lever rule [12].

The temperature of the start of the α → γ transformation was determined from the moment of simultaneous appearance of two effects, i.e., a dilatometric one (inflection in the curve $\Delta L - T$) associated with decrease in the linear sizes of the sample upon formation of a more compact crystal lattice of austenite and a thermal one ($\Delta T - T$) associated with emergence of temperature difference between the sample and the heater as a result of absorption of a part of the thermal energy of the sample (Fig. 1*a*). The temperature of the end of the transformation (Ac_3) was determined from the moment of detachment of the tangent from the linear region of the dilatometric curve, which corresponds to a totally austenitic condition of the steel (Fig. 1*a*).

The behavior of the dilatometric curve in the range of the phase transition (Fig. 1*a*) reflects the kinetics of the α → γ transformation (Fig. 1*b*). The positive direction of the peaks of the derivative indicates increase in the content of austenite. The derivative of the kinetic curve behaves similarly to the derivative of the dilatometric curve where the arrangement of the peaks on the temperature scale is concerned [13], and may be used for analysis of the processes of phase transition. When making the analysis, we decomposed the derivative of the kinetic curve into individual peaks using Gaussian curves with asymmetry. The hardness was measured using an

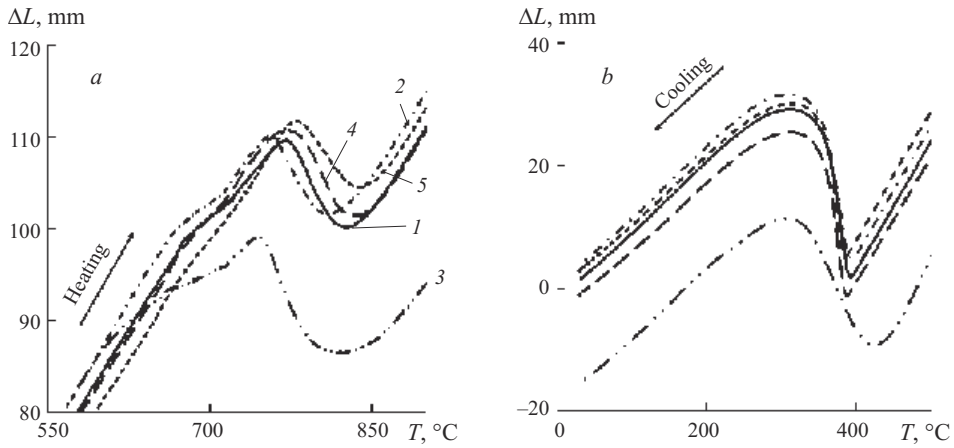

Fig. 2. Dilatometric curves of quenching of cold-deformed steel 10Kh2G3MFS from 1000°C in the ranges of formation of austenite (*a*) and martensite (*b*) for the following heating rates: *1*) 0.15 K/sec; *2*) 0.6 K/sec; *3*) 1.5 K/sec; *4*) 20 K/sec; *5*) 90 K/sec.

IT 5010 device at a load of 5 kgf by the Vickers method according to GOST 2999–75.

The microstructure was studied for the samples heat treated in the dilatometer. The microsections were prepared by the standard method by grinding against emery papers with different grain sizes (R240 – R2000) and then polishing with a diamond paste of fraction 1 – 2 μm. The surfaces of the microsections were etched by immersing them into a 4% alcoholic solution of nitric acid. The microstructure was studied under a Hitachi S-3400N scanning electron microscope at a magnification of up to × 5000 and an accelerating voltage of 20 kV. We determined the sizes of the ferrite and martensite regions by the intercept method using SIAMS firmware.

Specimens of type III-7 (GOST 1497–84) were tested for uniaxial tension in a REM-200-M-1 machine with "M-Test" software. The results of the tests for uniaxial tension were used to determine the work A_e in the range of uniform deformation, i.e.,

$$A_e = \frac{1}{3}\varepsilon_r(\sigma_{0.2} + 2\sigma_r), \quad (1)$$

where $\sigma_{0.2}$ is the conventional yield strength, MPa; σ_r is the ultimate strength, MPa; and σ_r is the strain in the region from the conventional yield strength to the ultimate strength determined by the method of [14].

The performance capability of steel 10Kh3G3MFS was assessed in terms of two criteria, i.e.,

– the criterion of the energy capacity W_c in tension [15]

$$W_c = \frac{\sigma_{0.2} + \sigma_r}{2} \ln\frac{1}{1-\psi}, \quad (2)$$

where ψ is the coefficient of contraction equal to 1/100 of the value of the contraction, and

– the criterion K_{cp} of crack propagation under tension

$$K_{cp} = 0.75W_c/\sigma_{0.2}. \quad (3)$$

The impact toughness (KCT) was determined for specimens with a crack of type 17 (GOST 9454–78) using an Instron CEAST 9350 electromechanical impactor bench. The *KCT* was chosen as a criterion of reliability because the steel has to serve under the conditions of dynamic loading and presence of stress concentrators in the form thread or crack-like defects.

RESULTS AND DISCUSSION

Formation of Austenite under Continuous Heating

Continuous heating above the temperature of the start of polymorphic transformation is a necessary part of isothermal treatment of the steel in the ICTR. The rate of the heating to the ICTR affects substantially the degree of the recrystallization of the matrix α-phase [16] and hence the position of the critical points and the kinetics of formation of austenite.

In the continuous heating in the ICTR the dilatometric curve exhibits two inflection points dividing the curves into three regions (Fig. 2*a*). During the heating in the bottom part of the ICTR (the first region of the dilatometric curve) expansion of the matrix α-phase prevails over compression due to the $\alpha \rightarrow \gamma$ rearrangement of the crystal lattice. The second region of the curve characterizes the occurrence of the main part of the transformation and takes a narrow temperature range. The slow growth of the content of austenite at the start of the $\alpha \rightarrow \gamma$ transformation and the displacement of its main part toward higher temperatures is illustrated by the kinetic curve for the heating rate of 1.5 K/sec (Fig. 1*b*). The content of the austenite formed in the bottom part of the ICTR decreases with increase of the heating rate from 0.15 to

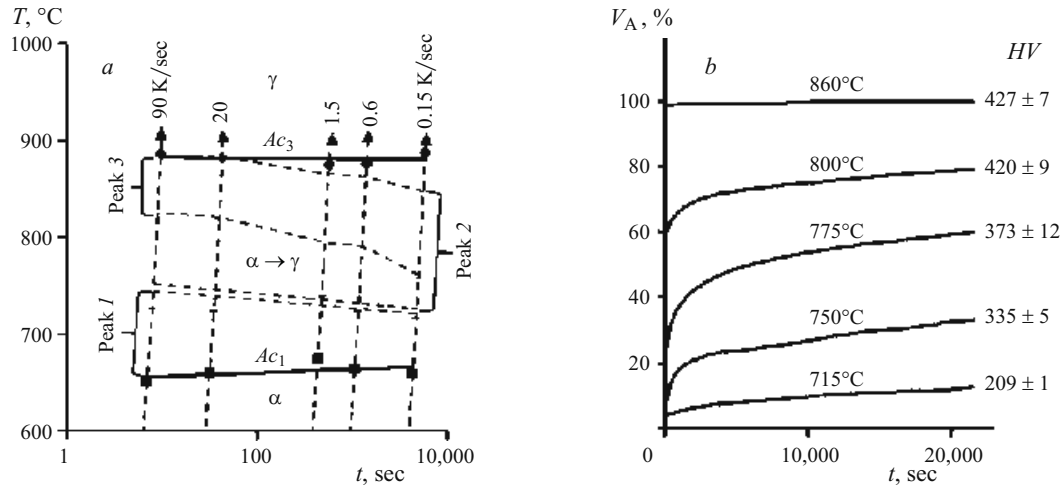

Fig. 3. Curves of formation of austenite in radially forged steel 10Kh3G3MFS: *a*) thermokinetic diagram (the heating rates are given at the vertical lines); *b*) kinetic curves of α → γ transformation at 715 – 860°C in 6-h hold (the hardness of the treated specimens is given on the right of the curves).

90 K/sec (Table 1). During the subsequent cooling, steel 10Kh3G3MFS undergoes a martensitic transformation at 400 ± 15°C and at 448°C for the heating rates of 0.6 – 90 and 0.15 K/sec respectively (Fig. 2*b*).

Analysis of the derivative of the kinetic curve gives us a notion of the variation of the rate of the α → γ transformation under continuous heating and allows us to distinguish three processes corresponding to peaks *1 – 3* (Fig. 1*b*). Each peak matches its own temperature range and the temperature T_{max} (Table 1) corresponding to the maximum rate of formation of austenite. The area under the peaks characterizes the contribution of the process into the total share of the formed austenite (parameter χ in Table 1).

When the heating rate is increased from 0.15 to 90 K/sec, the temperature ranges of peaks *1* and *2* grow and that of peak *3* is halved (Fig. 2*a*). The positions of the maximums of the rate of the transformation on the temperature scale change as follows: shift somewhat upward for peak *1* and shift toward higher temperatures by 45 and 30°C for peaks *2* and *3* respectively. It is important that the process corresponding to peak *2* plays a determining role in the austenitization, which is typical for heating of the steel in the initial high-tempered condition [13]. Its contribution into the development of the phase transformation increases from 69% to 88% with increase of the heating rate from 0.15 to 20 K/sec and is preserved at the level attained up to the heating rate of 90 K/sec. With increase of the heating rate, the proportion of the first process in the austenitization of the steel changes inconsiderably, and the contribution of the third process falls from 21 to 4%.

The effect of the heating rate on the critical points of steel 10Kh2G3MFS is reflected in the thermokinetic diagram of austenitization (Fig. 3*a*). The start of the transformation Ac_1 occurs in the temperature range 651 – 674°C, where the value of Ac_1 exhibits a weak tendency to lower with increase of the heating range. The α → γ transformation finishes at 881 ± 6°C.

TABLE 1. Quantitative Characteristics of Stages of α → γ Transformation at Various Heating Rates

v, K/sec	Parameters of the derivate of the kinetic curve								
	Stage *1*			Stage *2*			Stage *3*		
	T_{max}, °C	χ, %	V_A, %	T_{max}, °C	χ, %	V_A, %	T_{max}, °C	χ, %	V_A, %
0.15	690	10	9	765	69	41	821	21	86
0.6	697	9	8	778	82	46	834	9	95
1.5	703	8	5	790	86	41	834	6	92
20	701	6	1	805	88	50	850	6	95
90	699	9	1	812	87	52	851	4	93

Notations: T_{max} is the temperature at the maximum of the transformation rate; χ is the proportion of area under the peak; V_A is the content of austenite by the moment of attainment of maximum transformation rate.

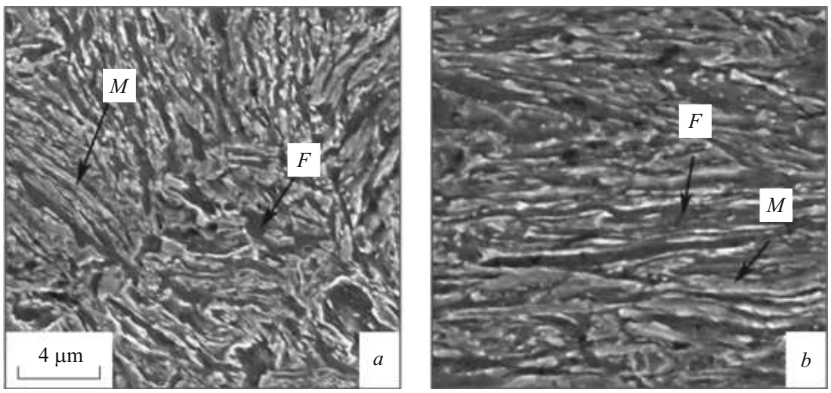

Fig. 4. Microstructure (SEM) of cold-deformed steel 10Kh3G3MFS in transverse (*a*) and longitudinal (*b*) sections of specimens.

Formation of Austenite under Isothermal Conditions

Formation of austenite under isothermal holds in the ICTR is characterized by kinetic curves (Fig. 3*b*). We chose the heating temperatures with allowance for the determined temperature maximums of the derivative of the kinetic curve under continuous heating at a rate of 1.5 K/sec. In this case, the structure of the steel contains some austenite (is given on the ordinate axis in Fig. 3*b*) by the moment of the start of the hold; its content is the higher the higher the heating temperature. Thus, the degree of the development of the $\alpha \rightarrow \gamma$ transformation under the isothermal hold depends on the content of the α-phase at the start of the hold and on the hold temperature, which serves the thermodynamic potential for implementation of the phase transformation. The $\alpha \rightarrow \gamma$ transformation damps down with time promoting preservation of the α-phase in the structure. It should be noted that the highest content of austenite forms under the isothermal conditions at 775°C. Increase of the temperature of the isothermal hold in the ICTR promotes development of the $\alpha \rightarrow \gamma$ transformation and growth of the hardness of the steel (Fig. 3*b*).

Formation of Structure under Quenching in ICTR

The preliminary cold radial forging produce in steel 10Kh2G3MFS a two-phase structure (Fig. 4) represented by ferrite regions with particles of carbides and martensite. In the cross section, the boundaries of the structural regions are somewhat curved (Fig. 4*a*). The longitudinal section presents a chiefly banded structure with alternating martensite and ferrite regions containing carbide particles (Fig. 4*b*).

A special feature of the changes during heating of cold-deformed steels is recrystallization of the matrix α-phase before or after formation of austenite [17 – 19]. Figure 5 presents the results of the structural analysis of steel 10Kh3G3MFS after quenching from different temperatures within the ICTR. It can be seen that the heating and holding in the lower part of the ICTR (715°C) produces new grains of the matrix α-phase. Several regions of martensite and numerous carbides are present in the structure over grain boundaries and in grain bodies against the background of a fine structure with recrystallized grains of the matrix α-phase (Fig. 5*a*). Inside the grains, the carbide particles are arranged in chains reflecting the location of the earlier existing substructural boundaries. The fine martensite regions have a lighter color and are observable at the junctions of several ferrite grains.

The microstructure of the steels quenched from 750, 775 and 800°C illustrates the occurrence of the second stage of formation of austenite, i.e., formation of new grains and their growth (Fig. 5*b* – *d*). After the quenching from 750°C, the number of the regions of transformed austenite increases noticeably (Fig. 5*b*) and they contain substructural components inside. The average size of the martensite regions is 2.8 ± 0.13 μm; that of the ferrite regions is 3.63 ± 0.18 μm. The content of the carbide phase decreases. Increase of the temperature of heating for quenching to 775°C causes higher dissolution of carbides and growth in the volume fraction of transformed austenite. The regions with martensitic structure consist of smaller regions differing in the orientation of the α-laths and separated by the boundaries of the initial austenite grains (Fig. 5*c*).

After the quenching from 800°C (Fig. 5*d*), martensite becomes the dominant structural component, and the size of its regions grows to 4.2 ± 0.27 μm. Quenching from 860°C gives a fully martensitic structure (Fig. 5*e*), which is confirmed by the data of the dilatometric analysis (Fig. 3*b*). The determined dependence of the sizes of the regions of the two-phase structure on the heating temperature (Fig. 6*a*) reflects preservation of the high fineness of the martensite regions in the holds at 715 – 800°C. At the same time, the total contents of the martensite and of the retained austenite increase in this temperature interval (Fig. 3*b*).

The earlier discovered fact [10] of abnormal stabilization of the grain size in the hold at 800°C upon prolongation of the hold from 15 to 125 min requires explanation. It should be noted that the temperature of 800°C under the conditions of continuous heating belongs to the region of the main maximum of the transformation rate (Table 1). The presence of a high content of α-phase in the structure (over 40%) during the hold promotes more intense formation of austenite, which has been detected in the quenching from 775°C (Fig. 5), and growth of the average grain size with prolonga-

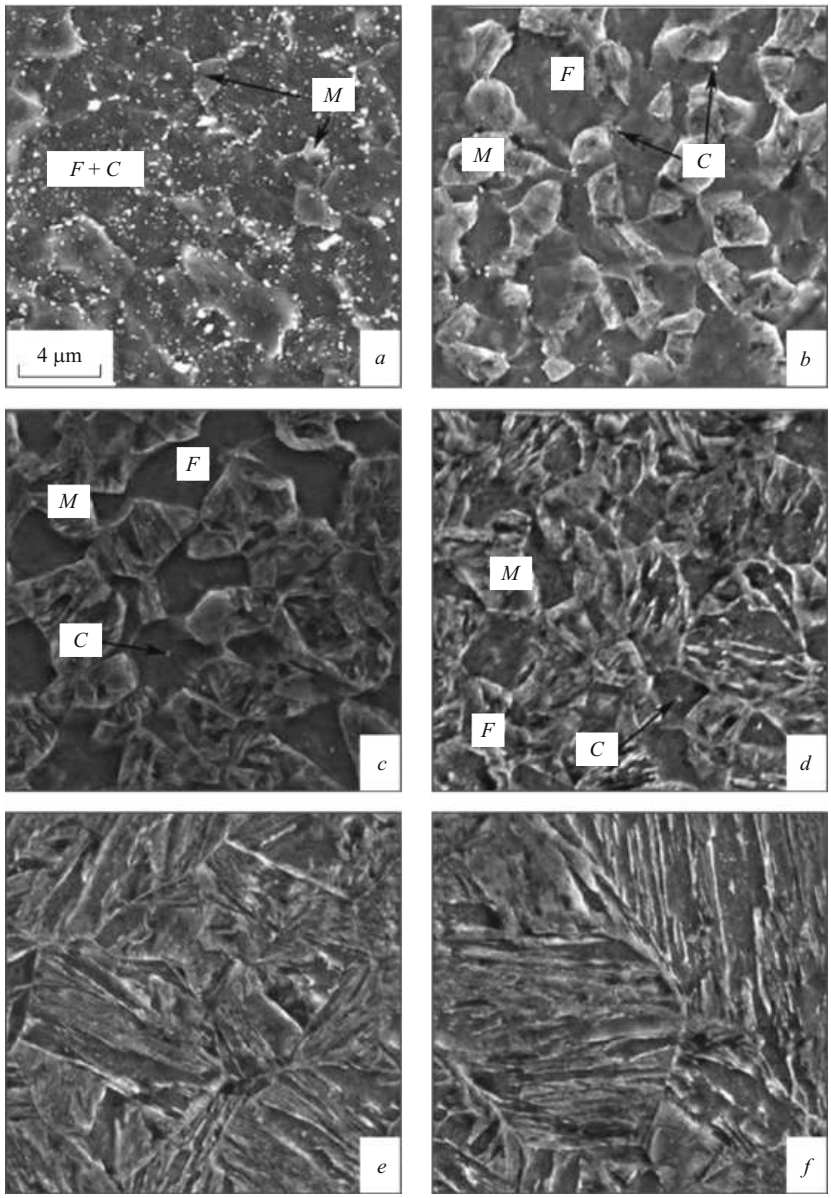

Fig. 5. Microstructure (SEM) of cold-deformed steel 10Kh3G3MFS after cold radial forging and quenching from the intercritical temperature range (with 6-h hold) from 715°C (*a*), 750°C (*b*), 775°C (*c*), 800°C (*d*), and 860°C (*e*, *f*).

tion of the hold from 15 to 125 min [10]. When the content of the α-phase in the structure is less than 20% (after a 6-h hold at 800°C), the growth of the content of austenite is accompanied by increase of the average size of the martensite regions (Fig. 6*a*).

Mechanical Properties

It has been shown that technological inheritance affects substantially the behavior of the curves of uniaxial tension of steel 10Kh3G3MFS (Fig. 6*b*). For the steel quenched from the temperature of complete austenitization from the ICTR (curves *1* and *2* in Fig. 6*b*, respectively), the stress-strain curves do not have a well manifested yield plateau, and the regions of lumped plastic strain have close lengths. The steel subjected to cold radial forging (curve *3* in Fig. 6*b*) acquires a high-strength condition characterized by absence of a region of uniform strain in the uniaxial tension curve. Determination of the conventional yield limit by the method of GOST 1497 is incorrect because the curve is intersected by a straight line parallel to the region of elastic deformation in the region of lumped strain. Quenching from the ICTR of the steel subjected to CRF (curves *4a* and *4b* in Fig. 6*b*) increases the range of uniform plastic strain in the uniaxial tension curve.

Increase of the temperature of heating of the cold-deformed steel in the ICTR from 775 (mode *4a*) to 800°C (mode *4b*) promotes growth of the conventional yield strength and of the ultimate strength by 7% (by 70 MPa) and of the impact toughness (*KCT*) by 10% (Table 2). The energy capacity of fracture W_c increases by 10% at close values of the crack growth criterion, which becomes the highest as compared to the same parameters of the steel in other condi-

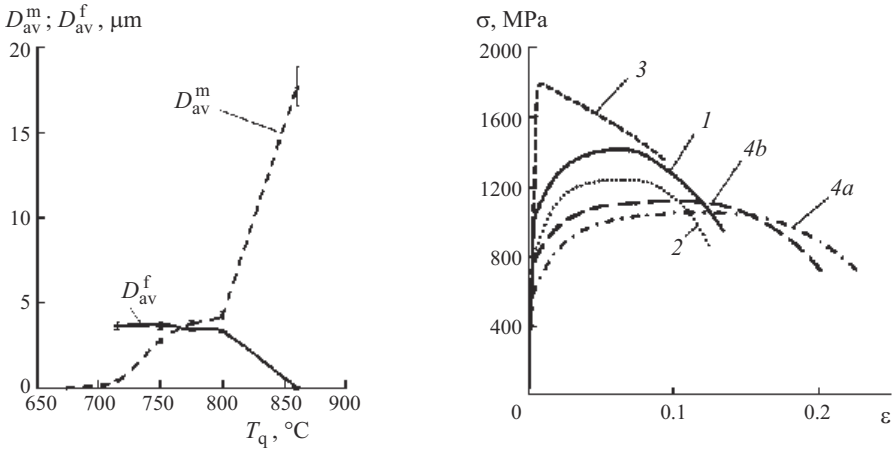

Fig. 6. Average grain size of martensite (D_{av}^{m}) and ferrite (D_{av}^{f}) as a function of the quenching temperature (6-h hold) (*a*) and stress-strain curves of steel 10Kh3G3MFS in different states: *1*) quenching from 950°C; *2*) mode *1* + quenching from 800°C for 2 h; *3*) mode *2* + cold radial forging to 60% deformation; *4a*) mode *3* + quenching from775°C for 2.1 h; *4b*) mode *3* + quenching from 800°C for 2.1 h.

tions. The contraction remains unchanged. The work of uniform deformation A_e decreases by 3%, which results in decrease of the elongation by 11%. By the data of the dilatometric analysis, increase of the heating temperature to 800°C raises the content of austenite in the structure from 54 to 79%, which means that the proportion of "fresh" martensite increases too. In addition, in accordance with [10], the average grain size in the steel is reduced.

The mechanical properties of the steel formed by incomplete quenching from 800°C are determined by its initial condition. The difference in the ultimate tensile strengths of the quenched and radially forged steel after the same modes of incomplete quenching (states *2* and *4b* in Table 2) is a result of the difference in the phase compositions and structural features of the untransformed α-phase. The content of the untransformed α-phase in state *4b* is 26%. By the data of the metallographic analysis, this phase undergoes recrystallization, which is sure to lower the density of crystal structure defects in it. The decrease in the number of defects in the α-phase should promote free sliding of dislocations raising the possibility of uniform deformation. In state *2*, the structure preserves 20% α-phase. The shape of the α-phase is close to that of the initial lath martensite and is fragmented additionally by dislocation subboundaries [9]. The growth in the content of the untransformed α-phase and the changes in its substructure cause lowering of the ultimate strength by 20 MPa and of the conventional yield strength by 80 MPa at 5% growth of the contraction, 17% growth of the work of uniform deformation A_e, 34% growth of the impact toughness and 9% growth of the crack growth criterion. The initial state before the incomplete quenching produces the strongest effect on the elongation, the value of which in state *4b* is higher than in state *2* by a factor of 1.67.

Such growth in the ductility of the steel is explainable by the structure of the matrix α-phase and possible manifestation of the TRIP-effect [20]. Preservation of some retained austenite in the structure of steel 10Kh3G3MFS has been detected in [9]. The stability of the retained austenite depends on the content of carbon in the γ-solid solution. In accordance with the Fe – C phase diagram, increase of the temperature of heating in the ICTR is accompanied by growth of the content of austenite in the structure and lowering of the carbon content in the austenite. By the end of the hold at 800°C, the preliminarily radially-cold-forged steel contains less austenite than the preliminarily quenched steel. Therefore, the carbon content in the austenite of the radi-

TABLE 2. Mechanical Properties and Criteria of Operability of Steel 10Kh3G3MFS in Different States

State*	Phase composition**	$\sigma_{0.2}$, MPa	σ_r, MPa	δ, %	ψ, %	A_e, J/m^3	W_c, MJ/m^3	K_{cp}, MPa^2	*KCT*, MJ/m^2
1	100% *M*	1100	1420	13.0	59	74	1111	0.76	0.44
2	80% ($M + A_{ret}$), 20% *F* [9]	910	1240	12.0	59	76	966	0.79	0.76
3	80% ($M_q + M_{def}$), 20% *F* [11]	–	1860	9.0	45	0	–	–	0.23
4a	52% ($M + A_{ret}$), 48% *F*	760	1050	22.5	62	102	866	0.85	0.93
4b	74% ($M + A_{ret}$), 26% *F*	830	1120	20.0	62	89	953	0.86	1.02

* See Fig. 6*b*.

** According to the data of the dilatometric analysis.

Notations: M) martensite; A_{ret}) retained austenite; *F*) untransformed α-phase (ferrite); A_e) work in the range of uniform deformation; W_c) empirical criterion of the energy capacity under tension; K_{cp}) criterion of crack propagation under tension; *KCT*) specific energy of crack propagation.

ally-cold-forged steel should be higher. In addition, by the data of the metallographic analysis, the content of the carbide phase in steel 100Kh3G3MFS changes actively during the treatment in the ICTR, which affects substantially the variation of the carbon concentration in the γ-phase. For example, it has been shown in [21] that continuous heating of a medium-carbon steel in the upper part of the ICTR is accompanied by dissolution of the carbide phase and growth of both the content of the forming austenite and of the carbon content in the latter. Thus, we may expect that preliminarily radially-cold-forged steel will preserve somewhat more retained austenite after the treatment from the ICTR than the quenched steel due to stabilization of the retained austenite caused by carbon enrichment.

It should be noted that the retained austenite is steel 10Kh2G3MFS is state *2* exhibits a high strain resistance, i.e., is preserved in the structure after an up to 40% deformation by the method of CRF [11].

CONCLUSIONS

We have studied the effect of cold radial forging of steel 10Kh3G3MFS in a two-phase martensitic-austenitic condition on the special features of formation of austenite and mechanical properties after quenching from the intercritical temperature range (ICTR). The temperature interval of formation of austenite in radially forged steel 10Kh3G3MFS widens upon increase of the heating rate from 0.15 to 90°C due to the lowering of the critical point Ac_1. For all the heating rates studied, we determined the temperature ranges of three stages of the α → γ transformation and the temperature of the main maximum of the rate of formation of γ-phase, which grows from 765 to 812°C upon increase of the heating rate; this results in formation of the main part of austenite in the middle and upper parts of the ICTR. The low rate of the α → γ transformation in the lower part of the ICTR (715 – 775°C) under continuous heating determines a low initial content of γ-phase under isothermal holds and a high fraction of isothermally formed austenite (77 – 89%) on the boundaries of the new set of grains of recrystallized α-phase, which have a size of 2.8 – 4.2 μm in the hold range of 750 – 800°C. It should be noted that the temperature of incomplete quenching (800°C) of radially forged steel 10Kh3G3MFS determined earlier in experiments corresponds to the highest value of the impact toughness *KCT* and is located in the region of the main maximum of the rate of the α → γ transformation; in addition to the recrystallization of the matrix α-phase, this causes formation of a very fine structure of polyhedral morphology with 75% martensite. As compared to the martensitic-ferritic structure with lath morphology obtained after the same treatment of quenched steel 10Kh3G3MFS, such a structure provides higher reliability characteristics, i.e., an elongation higher by a factor of 1.5 and an impact toughness *KCT* higher by 30%, while the ultimate tensile strength decreases by only 10%.

The work has been performed with financial support of the Government of the Perm Region within scientific project No. S 26/513.

REFERENCES

1. Yu. N. Simonov, M. Yu. Simonov, D. N. Poduzov, et al., "Transformations, structure and properties of system-alloyed low-carbon nickel-free steels," *Metalloved. Term. Obrab. Met*., No. 11(689), 4 – 11 (2012).
2. L. M. Kleiner, D. M. Larinin, L. V. Spivak, and A. A. Shatsov, "Phase and structural transformations in low-carbon martensitic steels," *Fiz. Met. Metalloved*., **108**(2), 161 – 168 (2009).
3. D. O. Panov and A. I. Smirnov, "Special features of formation of austenite in low-carbon steel under heating in the intercritical range," *Fiz. Met. Metalloved*., **118**(11), 1138 – 1148 (2017).
4. L. Ts. Zayats, D. O. Panov, Yu. N. Simonov, et al., "Special features of processes of formation of austenite in the intercritical temperature range in initially quenched low-carbon steels with different alloying systems," *Fiz. Met. Metalloved*., **112**(5), 505 – 513 (2011).
5. D. O. Panov, Yu. N. Simonov, P. A. Leont'ev, et al., "A study of phase and structural transformations of quenched low-carbon steel under the conditions of multiple intense thermal impact," *Metalloved. Term. Obrab. Met*., No. 11(689), 28 – 32 (2012).
6. D. O. Panov, A. N. Balakhnin, M. G. Titova, et al., "Evolution of the structure and properties under intense thermocycling treatment of cold-deformed quenched system-alloyed steel 10Kh3G3MF," *Metalloved. Term. Obrab. Met*., No. 11(689), 17 – 22 (2012).
7. A. S. Ermolaeva, M. G. Zakirova, L. M. Kleiner, and Yu. N. Simonov, "Structure and properties of low-carbon martensitic steels quenched from the intercritical temperature range," *Konstr. Komp. Mater.*, No. 4, 172 – 177 (2006).
8. Yu. N. Simonov, M. Yu. Simonov, D. O. Panov, et al., "Formation of structure of lower carbide-free bainite due to isothermal treatment of steels of type Kh3G3MFS and KhN3MFS," *Met. Sci. Heat Treat*., **58**(1 – 2), 61 – 79 (2016). DOI: 10.1007/s11041-016-9965-z
9. D. O. Panov, T. Yu. Barsukova, A. I. Smirnov, et al., "Intercritical quenching of low-carbon steels with formation of a fine multiphase structure," *Obrab. Met. (Tekhnol., Oborud., Instr.)*, No. 4(77), 6 – 18 (2017). DOI: 10.17212/1994-6309-2017-4-6-18
10. T. Yu. Barsukova, D. O. Panov, and Yu. N. Simonov, "Laws of formation of structure and properties in cold-deformed low-carbon structural steel under incomplete quenching," *Metalloved. Term. Obrab. Met*., No. 7, 3 – 9 (2021).
11. T. Yu. Barsukova, D. O. Panov, A. S. Pertsev, et al., "Evolution of the structure and properties of multiphase low-carbon steel during cold radial forging," *Metalloved. Term. Obrab. Met*., No. 10(772), 25 – 32 (2019).
12. L. I. Gladshtein, T. N. Rivanenok, and A. V. Khristov, "Dilatometric analysis of the kinetics of polymorphic transformation under heating," *Zavod. Lab., Diagn. Met*., **74**(6), 36 – 39 (2008).
13. T. Yu. Barsukova, D. O. Panov, and M. Yu. Simonov, "Formation of superfine-grained ferritic-martensitic structure in

low-carbon structural steel in quenching from intercritical temperature range," *Tekhnol. Met*., No. 11, 2 – 12 (2019).
14. S. K. Greben'kov, A. A. Shatsov, D. M. Larinin, and L. M. Kleiner, "Deformation hardening of low-carbon martensitic steels," *Metalloved. Term. Obrab. Met*., No. 2, 33 – 38 (2016).
15. S. K. Greben'kov, V. A. Skudnov, and A. A. Shatsov, "Deformation and fracture of low-carbon martensitic steels," *Metalloved. Term. Obrab. Met*., No. 2, 33 – 38 (2016).
16. A. Chbihi, D. Barbier, L. Germain, et al., "Interactions between ferritic recrystallization and austenite formation in high-strength steels," *J. Mater. Sci*., **49**(10), 3608 – 3621 (2014). DOI: 10.1007/s10853-014-8029-2
17. D. O. Panov, Yu. N. Simonov, L. V. Spivak, and A. I. Smirnov, "Stages of austenitization of cold-deformed low-carbon steel in intercritical temperature range," *Fiz. Met. Metalloved*., **116**(8), 846 – 853 (2015).
18. M. Tokizane, N. Matsumura, K. Tsuzaki, et al., "Recrystallization and formation of austenite in deformed lath martensitic structure of low carbon steels," *Metall. Trans. A*, **13**, 1379 – 1388 (1982). DOI: 10.1007/BF02642875
19. J. Huang, W. J. Poole, and M. Millitzer, "Austenite formation during intercritical annealing," *Metall. Mater. Trans*., **35**(11), 3363 – 3375 (2004).
20. E. Tesser, C. Silva, A. Artigas, and A. Monsalve, "Effect of carbon content and intercritical annealing on microstructure and mechanical tensile properties in FeCMnSiCr TRIP-assisted steels," *Metals*, **11**(10) (2021). DOI: 10.3390/met11101546
21. M. A. Gervas'ev, A. S. Yurovskikh, S. V. Belikov, et al., "Effect of Al and Si on formation of austenite in intercritical temperature range of Cr – Ni – Mo-steel," *Chern. Metall*., **58**(9), 677 – 681 (2015).